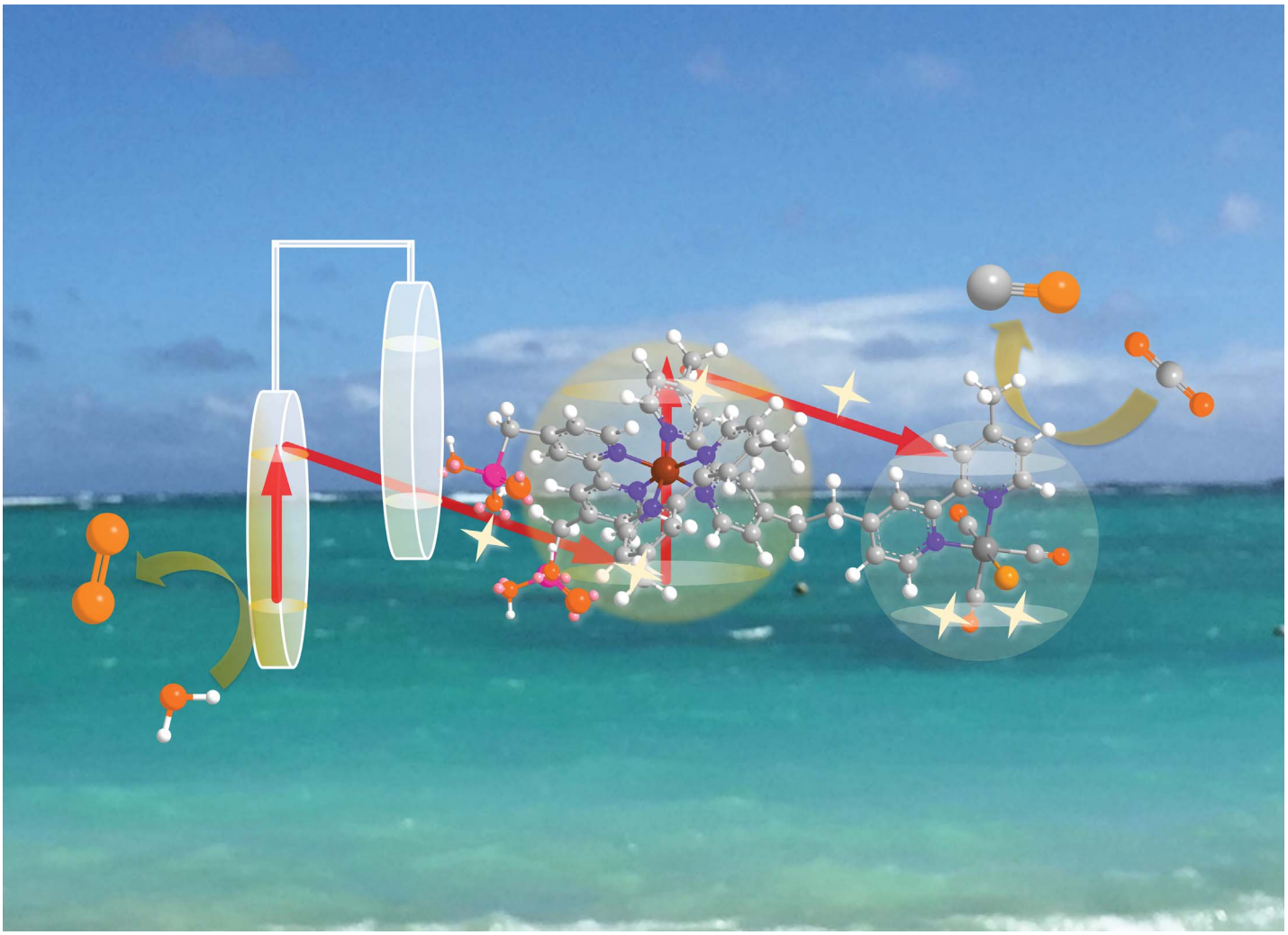

Showcasing research from Osamu Ishitani's laboratory, Department of Chemistry, Tokyo Institute of Technology, Japan.

Hybrid photocathode consisting of a $CuGaO_2$ p-type semiconductor and a Ru(II)–Re(I) supramolecular photocatalyst: non-biased visible-light-driven CO_2 reduction with water oxidation

A $CuGaO_2$ p-type semiconductor electrode was successfully employed for constructing a new hybrid photocathode with a Ru(II)–Re(I) supramolecular photocatalyst (RuRe/$CuGaO_2$) for the conversion of CO_2 to CO in an aqueous electrolyte solution. With the aid of a positive onset potential of +0.3 V *vs.* Ag/AgCl of this RuRe/$CuGaO_2$ photocathode, a photoelectrochemical cell comprising the RuRe/$CuGaO_2$ photocathode and a CoO_x/TaON photoanode demonstrated the visible-light-driven catalytic reduction of CO_2 using water as a reductant without applying any external bias, as the first instance of the self-driven system constructed with the molecular photocatalyst.

As featured in:

See Osamu Ishitani *et al.*, *Chem. Sci.*, 2017, **8**, 4242.

ROYAL SOCIETY OF CHEMISTRY

rsc.li/chemical-science

Registered charity number: 207890

Chemical Science

EDGE ARTICLE

View Article Online
View Journal | View Issue

Cite this: *Chem. Sci.*, 2017, **8**, 4242

Hybrid photocathode consisting of a $CuGaO_2$ p-type semiconductor and a Ru(II)–Re(I) supramolecular photocatalyst: non-biased visible-light-driven CO_2 reduction with water oxidation†

Hiromu Kumagai,[a] Go Sahara,[a] Kazuhiko Maeda,[a] Masanobu Higashi,[b] Ryu Abe[b] and Osamu Ishitani*[a]

Received 1st March 2017
Accepted 5th April 2017

DOI: 10.1039/c7sc00940b

rsc.li/chemical-science

A $CuGaO_2$ p-type semiconductor electrode was successfully employed for constructing a new hybrid photocathode with a Ru(II)–Re(I) supramolecular photocatalyst (**RuRe**/$CuGaO_2$). The **RuRe**/$CuGaO_2$ photocathode displayed photoelectrochemical activity for the conversion of CO_2 to CO in an aqueous electrolyte solution with a positive onset potential of +0.3 V *vs.* Ag/AgCl, which is 0.4 V more positive in comparison to a previously reported hybrid photocathode that used a NiO electrode instead of $CuGaO_2$. A photoelectrochemical cell comprising this **RuRe**/$CuGaO_2$ photocathode and a CoO_x/TaON photoanode enabled the visible-light-driven catalytic reduction of CO_2 using water as a reductant to give CO and O_2 without applying any external bias. This is the first self-driven photoelectrochemical cell constructed with the molecular photocatalyst to achieve the reduction of CO_2 by only using visible light as the energy source and water as a reductant.

Introduction

The use of artificial photosynthesis, particularly for the photochemical reduction of CO_2, has gained much attention because it might provide solutions for overcoming both the problem of global warming and the shortage of fossil resources. Metal complex photocatalysts have been intensively developed for achieving the reduction of CO_2 using the energy of visible light with a high selectivity for the products.[1–3] In particular, supramolecular photocatalysts composed of both redox photosensitizer and catalyst units have exhibited high selectivity, durability, and efficiency for the reduction of CO_2 under visible light conditions even in aqueous solutions,[4,5] as well as in organic solvents.[6–14] In these photocatalytic reactions, sacrificial reductants such as 1-benzyl-1,4-dihydronicotinamide,[7] sodium ascorbate,[4] and 2-(1,3-dimethyl-2,3-dihydro-1*H*-benzimidazol-2-yl)benzoic acid[5] are necessary because of the low oxidizing power of the photosensitizer unit, which cannot sufficiently oxidize water, an abundant electron donor.

Hybrid photocatalysts and photoelectrodes composed of metal complexes and semiconductor materials with relatively high photochemical oxidizing power, in which the metal complexes act as catalysts alone in some cases[15–24] but as photocatalysts in others,[25–30] have recently been studied for the visible-light-driven photocatalytic reduction of CO_2. In the cases where metal complexes are used as photocatalysts, hybrid photocatalysts with semiconductor particles can cope with both the high selectivity of the CO_2 reduction and the strong oxidation power *via* the step-by-step excitation of both the redox photosensitizer unit of the metal complex photocatalyst and the semiconductor, so-called *Z*-scheme mechanism. However, visible-light-driven CO_2 reduction accompanied by water oxidation has not been achieved yet using hybrids with these particle systems. We have previously reported a hybrid photocathode consisting of a Ru(II)–Re(I) supramolecular photocatalyst (**RuRe**) fixed on a NiO p-type semiconductor electrode for the photoelectrochemical reduction of CO_2.[31] In this system, the metal complex photocatalyst can drive the reduction of CO_2 by the injection of electrons from an external electric circuit through the NiO semiconductor electrode without the addition of any sacrificial electron sources. This **RuRe**/NiO photoelectrochemical system was used to successfully achieve the catalytic reduction of CO_2 using water as an electron source, combined with a CoO_x/TaON n-type semiconductor photoanode for the oxidation of water.[32] However, the performance of this photoelectrochemical cell was still insufficient, *i.e.*, the combined photoelectrochemical cell needed the assistance of an external electrical bias (0.3 V) and a chemical bias (0.10 V) produced by a difference in pH, and the photoelectrochemical cell generated much lower yields of the

[a]*Department of Chemistry, School of Science, Tokyo Institute of Technology, O-okayama 2-12-1-NE-1, Meguro-ku, Tokyo 152-8550, Japan. E-mail: ishitani@chem.titech.ac.jp*

[b]*Department of Energy and Hydrocarbon Chemistry, Graduate School of Engineering, Kyoto University, Katsura, Nishikyo-ku, Kyoto 615-8510, Japan*

† Electronic supplementary information (ESI) available. See DOI: 10.1039/c7sc00940b

reduction products (CO and H_2) compared to the oxidation one (O_2) from the viewpoint of electron balance.

One of the main reasons for these insufficiencies was the low activity of the NiO electrode. Although NiO has been widely used as an electrode material for p-type dye-sensitized photocathodes, the flat band position of NiO is relatively negative (+0.34 V *vs.* Ag/AgCl in a saturated aqueous solution of KCl at a pH of 7).[33] This could cause a large loss of energy for passing an electron to the excited state of the Ru(II) photosensitizer unit ($E_{1/2}$ = +0.51 V *vs.* Ag/AgCl)[31] through the interface, leading to the requirement of a large external bias (totally 0.4 V) when this photocathode is used for constructing a photoelectrochemical cell combined with a photoanode. The consumption of electrons for reducing trivalent nickel ions (Ni^{3+}) that originally existed in NiO could also be problematic because it lowers the Faraday efficiencies of the reduction reactions on the photocathode.[31,32,34] Therefore, the development of new p-type semiconductor electrodes is necessary for the field of hybrid photoelectrochemical cells with supramolecular photocatalysts for reduction of CO_2.

Here, we report a novel hybrid photocathode (**RuRe**/$CuGaO_2$) consisting of $CuGaO_2$ as the p-type semiconductor electrode and **RuRe** as the photocatalyst for the reduction of CO_2. $CuGaO_2$ with a delafossite crystal structure is known to exhibit p-type semiconducting properties that are derived from native Cu^+ vacancies.[35] It has received attention as a transparent conducting oxide material[36–38] and has also been studied as an alternative to NiO for dye-sensitized photocathodes due to both its high conductivity (10^{-1}–10^{-2} S cm^{-1})[38] and positive flat band potential, which was reported to be approximately 0.16 V more positive compared to that of NiO.[39,40] Although $CuGaO_2$ electrodes have been investigated as parts of dye-sensitized solar cells, to the best of our knowledge there are no reports on the application of $CuGaO_2$ electrodes for photocatalytic reactions such as CO_2 reduction and H_2 evolution. The onset potential for the reduction of CO_2 by the as-synthesized **RuRe**/$CuGaO_2$ was revealed to be 0.4 V more positive in comparison to that of the **RuRe**/NiO electrode. A photoelectrochemical cell consisting of **RuRe**/$CuGaO_2$ and a CoO_x/TaON photoanode enabled the visible-light-driven catalytic reduction of CO_2 using water as the reductant without applying any external bias.

Results and discussion

Preparation of the RuRe/$CuGaO_2$ photocathode

$CuGaO_2$ powder was prepared using a solid-state reaction method. The XRD pattern of the synthesized powder revealed that the delafossite structure of the $CuGaO_2$ was obtained with no obvious impurity phase (Fig. S1†). The UV-vis diffuse reflectance spectrum of the synthesized $CuGaO_2$ powder indicated that the powder absorbs light at λ < 460 nm, which has been reported in previous research into $CuGaO_2$ powder (Fig. S2†).[41,42] The $CuGaO_2$ electrodes were prepared by drop-casting a powder suspension onto FTO glass substrates following annealing with a N_2 flow. SEM observations revealed that the polycrystalline $CuGaO_2$ particles had rod-like shapes on the micron scale and the thickness of the stacked $CuGaO_2$ particle layer of the electrode was approximately 15 μm (Fig. S3†). The dominant material at the solid–liquid interface of the electrode should be the deposited $CuGaO_2$ particles and not the underlying flat FTO film. **RuRe** and its model complexes (**Ru** and **Re**) (see Chart 1) were synthesized in accordance with reported procedures.[43] A $CuGaO_2$ electrode was immersed in an acetonitrile solution containing the metal complex overnight to obtain hybridized photocathodes.

Photoelectrochemical properties of the RuRe/$CuGaO_2$ photocathode

The photoelectrochemical properties of the synthesized **RuRe**/$CuGaO_2$ electrode were investigated under irradiation at λ_{ex} > 460 nm, which can be selectively absorbed by the Ru photosensitizer unit of **RuRe**, in an aqueous solution containing $NaHCO_3$ (50 mM) saturated with CO_2, which was used as the supporting electrolyte. Fig. 1(a) shows the current–potential curves of the **RuRe**/$CuGaO_2$ electrode under continuous visible-light irradiation (λ_{ex} > 460 nm) and under dark conditions. This clearly indicates that the **RuRe**/$CuGaO_2$ electrode generated a cathodic photocurrent under irradiation. The difference in the observed current between the irradiation and dark conditions indicated that the cathodic photoresponse of the **RuRe**/$CuGaO_2$ electrode started at approximately +0.3 V *vs.* Ag/AgCl (equivalent to +0.9 V *vs.* RHE). It should be noted that this onset potential of the photocurrent was approximately 0.4 V more positive than that of **RuRe**/NiO (*ca.* −0.1 V, Fig. 1(b)).[31] A pristine $CuGaO_2$ electrode showed a slight cathodic photoresponse (*ca.* −1 μA cm^{-2}) under irradiation at λ_{ex} > 460 nm (Fig. S4†), which was almost negligible compared to the photocurrent from the **RuRe**/$CuGaO_2$ electrode, as shown in Fig. 1(a). The anodic current obtained from *ca.* +0.2 V *vs.* Ag/AgCl in the dark was derived from the self-oxidation of the $CuGaO_2$ surface[42] but not from the redox reaction of the immobilized **RuRe**.

Fig. 2 shows the dependence of the IPCE of the **RuRe**/$CuGaO_2$ electrode and a bare $CuGaO_2$ electrode without **RuRe** on the wavelength of light used for irradiation when the applied potential was −0.3 V *vs.* Ag/AgCl. The diffuse reflectance spectra of these electrodes are also shown in Fig. 2. The **RuRe**/$CuGaO_2$ electrode displayed light absorption up to 600 nm, which was derived from the **Ru** photosensitizer unit of the hybridized

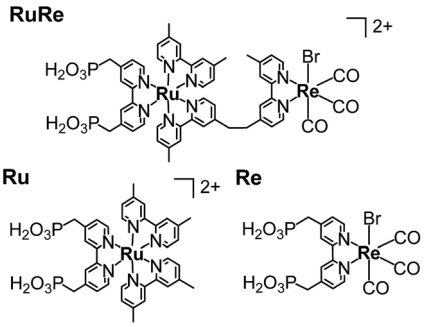

Chart 1 Structures and abbreviations of the Ru(II)–Re(I) supramolecular photocatalyst (**RuRe**) and its model mononuclear metal complexes used as the photosensitizer unit (**Ru**) and the catalyst unit (**Re**).

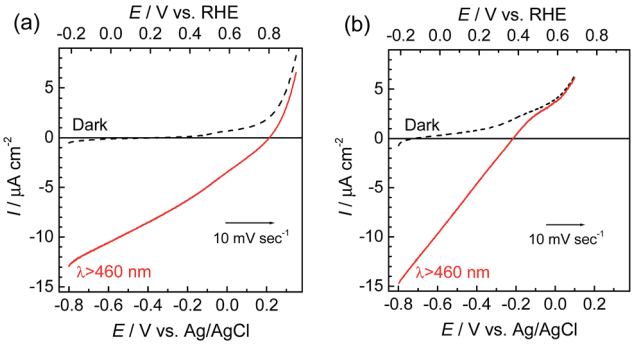

Fig. 1 Current–potential curves of **RuRe**/$CuGaO_2$ (a) and **RuRe**/NiO[31] (b) electrodes under continuous visible-light irradiation (λ_{ex} > 460 nm) and under dark conditions. A 50 mM aqueous solution of $NaHCO_3$ (pH 6.6) saturated with CO_2 was used as the electrolyte.

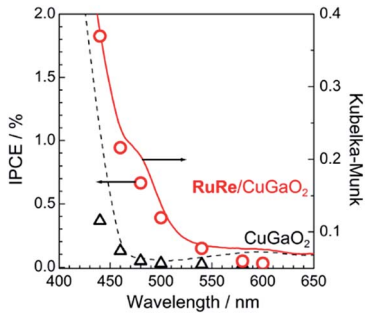

Fig. 2 Dependence on wavelength of the incident-photon-to-current efficiencies of the **RuRe**/$CuGaO_2$ (red circles) and bare $CuGaO_2$ (black triangles) electrodes at −0.3 V *vs.* Ag/AgCl. An aqueous solution containing 50 mM $NaHCO_3$ saturated with CO_2 was used as the electrolyte (pH 6.6). The diffuse reflectance spectra of these electrodes are also shown: **RuRe**/$CuGaO_2$ (red solid line) and $CuGaO_2$ (black broken line).

RuRe. In the case of the **RuRe**/$CuGaO_2$ electrode, the dependence agreed well with the absorption spectrum of the electrode, whereas the bare $CuGaO_2$ electrode exhibited almost no photoresponse under irradiation at λ_{ex} > 460 nm. The flat band potential of the $CuGaO_2$ electrode in the reaction solution was estimated using electrochemical impedance spectroscopy (Fig. S5†) to be +0.47 V, which was more negative than the reduction potential of the excited state of **RuRe** ($E^{*red}_{1/2}$ = +0.49 V).[44] These results obviously indicate that the photocurrent was induced by the injection of the electrons from the $CuGaO_2$ electrode into the excited Ru photosensitizer unit of **RuRe**, as shown in Fig. 3. To conclude this section, we successfully synthesized the new hybrid photocathode (**RuRe**/$CuGaO_2$) for the reduction of CO_2 with an onset potential that was approximately 0.4 V more positive in comparison to that reported for the **RuRe**/NiO photocathode.

Photoelectrochemical reduction of CO_2 using the RuRe/$CuGaO_2$ photocathode

The gas products were analyzed during the continuous visible-light irradiation (λ_{ex} > 460 nm) of the **RuRe**/$CuGaO_2$ photocathode in an aqueous solution saturated with CO_2 in the presence of an applied potential. Fig. 4 shows the time courses of both the produced CO and H_2, and a half amount of electrons passing at an applied potential of −0.3 V *vs.* Ag/AgCl. After irradiating for 15 h, 966 nmol of CO and 622 nmol of H_2 were detected as the reduction products when the turnover number for the formation of CO (TON_{CO}), which was based on the **RuRe** deposited on the electrode, was 125, and the total faradaic efficiency for the production of the reduced products (CO + H_2) was 81%. In the irradiated solution, HCOOH was not detected (the detection limit of the capillary electrophoresis system used was 2 μmol). An isotope tracer experiment using $^{13}CO_2$ and $NaH^{13}CO_3$ was also conducted to confirm the source of the carbon for the produced CO. GC-MS analysis using $NaH^{13}CO_3$ as the electrolyte under a $^{13}CO_2$ atmosphere revealed that ^{13}CO was the main product of the reaction with a very small proportion of ^{12}CO, where the ^{13}C content was 99% in both $^{13}CO_2$ and $NaH^{13}CO_3$ (Fig. 5(a)). It is worth noting that the Re unit of **RuRe** has three ^{12}CO ligands, and the exchange of the ^{12}CO ligands with ^{13}CO proceeded in the photocatalytic $^{13}CO_2$ reduction reactions in homogeneous systems. On the other hand, only ^{12}CO was detected in the gas phase of the reaction using ordinary CO_2 and $NaHCO_3$ (Fig. 5(b)). These results clearly indicate that the source of carbon for CO was CO_2.

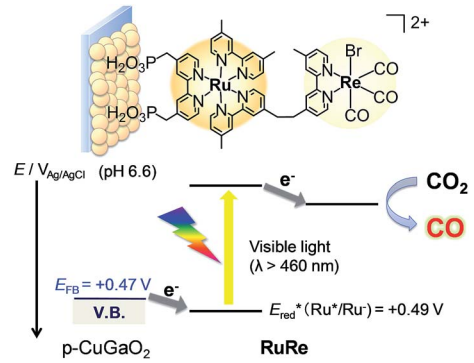

Fig. 3 Reaction scheme of the reduction of CO_2 by the **RuRe**/$CuGaO_2$ hybrid photocathode.

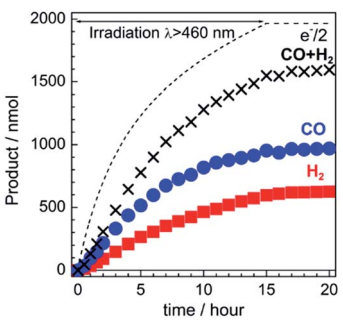

Fig. 4 Time courses of the chemical products (CO and H_2) and a half amount of electrons passing through the **RuRe**/$CuGaO_2$ photocathode under continuous visible-light irradiation (λ_{ex} > 460 nm) at −0.3 V *vs.* Ag/AgCl. A 50 mM aqueous solution of $NaHCO_3$ (pH 6.6) that was saturated with CO_2 was used as the electrolyte.

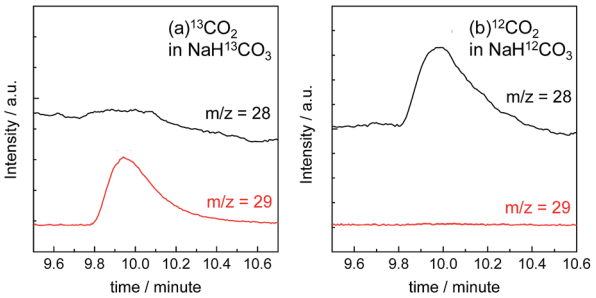

Fig. 5 GC-MS chromatograms of the gas products in the reaction chamber after irradiation (the detected $m/z = 28$ for ^{12}CO and 29 for ^{13}CO). The **RuRe**/$CuGaO_2$ photocathode was irradiated at λ_{ex} > 460 nm in an aqueous solution containing 50 mM sodium bicarbonate (pH 6.6) at −0.7 V *vs.* Ag/AgCl for 5 h using $^{13}CO_2$ and $NaH^{13}CO_3$ (a) and ordinary CO_2 and $NaHCO_3$ (b).

Table 1 shows the results of the photoelectrochemical reactions that were conducted under various conditions. The **RuRe**/$CuGaO_2$ electrode could produce CO as the main product with H_2 under visible-light irradiation at an applied potential from −0.1 V to −0.7 V *vs.* Ag/AgCl (Table 1, entries 1–3). The TON_{CO} of the **RuRe**/$CuGaO_2$ electrode was more than twice the reported value of the **RuRe**/NiO electrode (32; entry 10), even at more positive potentials, *i.e.*, −0.3 V and −0.1 V. Carbon monoxide was not produced under an Ar atmosphere even when the same photocathode was used, whereas H_2 was produced (entry 4). The reactions using the bare $CuGaO_2$ electrode or electrodes with only one of the model mononuclear complexes, *i.e.*, **Ru** or **Re**, did not lead to the formation of any CO (entries 5, 6, 7 and 8). In these cases, almost negligible or small amounts of H_2 were produced during the irradiation. Therefore, the $CuGaO_2$ electrode, the **RuRe** supramolecular photocatalyst, and a CO_2 atmosphere may all be required for the photoelectrochemical reduction of CO_2. We note that an electrode that was loaded with both the model complexes (**Re** and **Ru**) at random produced a much smaller amount of CO (entry 9), which indicates that the molecular design of **RuRe**, which enables the sufficiently efficient transfer of electrons from the reduced photosensitizer unit to the catalyst unit, is quite important for developing photocathodes for the reduction of CO_2.

As was described above, the production of H_2 was detected using the **RuRe**/$CuGaO_2$ photocathode in reactions under both Ar and CO_2 atmospheres, whereas only a small amount of H_2 was produced in the case of **RuRe**/NiO. It has been reported that the decomposition products of both the **Ru** photosensitizer unit in systems using **RuRe** supramolecular photocatalysts and **Ru** in a mixed system of **Ru** and **Re**, *i.e.*, a complex of the form $[Ru^{II}(N^N)_2(solvent)_2]^{n+}$ (N^N = diimine ligand), were gradually produced during the photocatalytic reactions, and these acted as catalysts for both the evolution of H_2 and the formation of HCOOH from CO_2.[5,45] However, the **Ru**/$CuGaO_2$ photocathode produced a smaller amount of H_2 than that of the **RuRe**/$CuGaO_2$ photocathode. Therefore, the generation of H_2 might result not only from the decomposition products of **RuRe** but also from the coexistence of photoexcited **RuRe** on the $CuGaO_2$ surface. Because it has been reported that $CuGaO_2$ worked as a H_2-evolving photocathode under UV light irradiation ($CuGaO_2$ itself can absorb UV light),[42] back electron transfer from photoexcited **RuRe** to the $CuGaO_2$ surface, which could act as an active site of H_2 evolution, might induce the production of H_2. Detailed studies of the reaction mechanism of the production of H_2 and its suppression are in progress in our laboratory.

Fig. 6 shows the time courses of the photocurrent using the **RuRe**/$CuGaO_2$ photocathode at the potentials of −0.1 V, −0.3 V, and −0.7 V *vs.* Ag/AgCl under irradiation at λ_{ex} > 460 nm, which correspond to entries 1–3 in Table 1. In all of the cases, a photocurrent was observed even after irradiation for 15 h. However, the photocurrent decreased in the first stage of the photoelectrochemical reaction, and the rates of formation of CO and H_2 also became slower in accordance with the decline in the photocurrent (Fig. 4 for the case at −0.3 V; Fig. S6† for the other cases). To confirm the reasons for the decline in the photocurrent and the rates of product formation, an estimation of the amount of "electrochemically active" **RuRe** species on the $CuGaO_2$ surface was conducted using cyclic voltammetry in an

Table 1 Photoelectrochemical reactions using various electrodes under various conditions[a]

				Products		
Entry	Sample	Complex/nmol	Potential[b]/V	CO/nmol (TON_{CO})	H_2/nmol	F_{red}[f]/%
1	**RuRe**/$CuGaO_2$	7.9	−0.7	668(85)	387	68
2	**RuRe**/$CuGaO_2$	7.7	−0.3	966(125)	622	81
3	**RuRe**/$CuGaO_2$	9.3	−0.1	781(84)	494	72
4[c]	**RuRe**/$CuGaO_2$	8.3	−0.3	n.d.[g]	346	52
5	$CuGaO_2$	—	−0.7	n.d.[g]	25	7
6	$CuGaO_2$	—	−0.3	n.d.[g]	Trace	—
7	**Ru**/$CuGaO_2$	9.6	−0.3	n.d.[g]	64	20
8	**Re**/$CuGaO_2$	14.2	−0.3	n.d.[g]	25	13
9[d]	(**Ru**,**Re**)/$CuGaO_2$	Re: 11.1, Ru: 4.4	−0.3	35(3, based on **Re**)	31	34
10[e]	**RuRe**/NiO[32]	11.2	−0.7	361(32)	36	64

[a] The electrode was irradiated at λ_{ex} > 460 nm using a 300 W Xe lamp for 15 h. A 50 mM aqueous solution of $NaHCO_3$ was used as the electrolyte. [b] Versus Ag/AgCl (sat. KCl). [c] Under an Ar atmosphere. [d] The electrode was prepared *via* immersion in solutions of **Re** and **Ru** in sequence. [e] Data from ref. 32 (irradiated for 12 h). [f] F_{red}: Faradaic efficiency for reduction reaction. [g] n.d.: not detected.

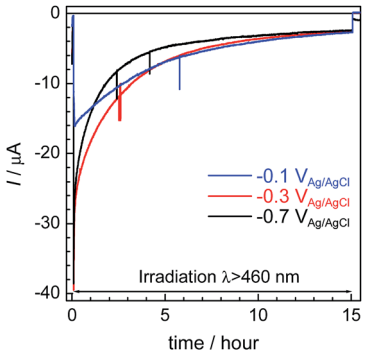

Fig. 6 Time courses of the photocurrent using the **RuRe**/$CuGaO_2$ photocathode at various potentials (corresponding to entries 1–3 in Table 1) under irradiation at λ_{ex} > 460 nm.

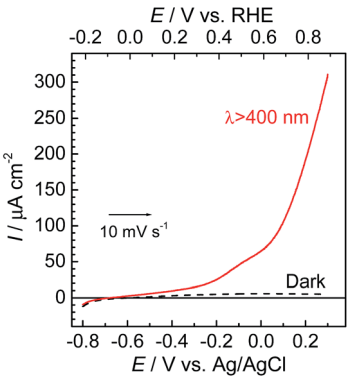

Fig. 7 Current–potential curves of the CoO_x/TaON photoanode under continuous visible-light irradiation (λ_{ex} > 400 nm) and under dark conditions. A 50 mM aqueous solution of $NaHCO_3$ (pH 6.6) saturated with CO_2 was used as the electrolyte.

acetonitrile solution (Fig. S7 and Table S1†) according to reported procedures, where the areas of the oxidation peaks of Ru^{II}/Ru^{III} were used for the estimation.[32] This indicated that about 80% of the **RuRe** lost its electrochemical activity after reacting for 15 h, which was probably due to (photo)desorption and/or photodecomposition of **RuRe** and could account for the decline in the photocurrent and the photocatalytic activity. In addition, the difference between the peak potentials of the redox reaction of Ru^{II}/Ru^{III} was greater after the reaction (Fig. S7†), which indicates that the ohmic resistance of the electrode increased. Because the XPS measurements of the electrodes showed no obvious change in the electronic states of the Cu and Ga on the surface of the $CuGaO_2$ particles during the reaction (Fig. S8†), the increase in the internal resistance of the $CuGaO_2$ electrode might not be caused by the collapse of the $GuGaO_2$ surface. An increase in inter-particle resistance probably proceeded in the electrode owing to the gradual deterioration of physical contact among the $GuGaO_2$ particles. This might induce the deactivation of the photocathode. We note that the peaks of Ru and Re in the XPS measurements were too small to be identified, possibly due to the low loading density of **RuRe** on $CuGaO_2$.

Photoelectrochemical reduction of CO_2 using a hybrid electrochemical cell with a *Z*-scheme configuration

To couple the photoelectrochemical reduction of CO_2 to the oxidation of water, the CoO_x/TaON photoanode, which has been reported to be an efficient photoanode for the water oxidation reaction, was examined as the counter photoanode in a full photoelectrochemical cell using the **RuRe**/$CuGaO_2$ hybrid photocathode. The CoO_x/TaON electrode was prepared according to a previously reported method.[46] Fig. 7 shows the current–potential curve of the CoO_x/TaON photoanode in a 50 mM aqueous solution of $NaHCO_3$ with a pH of 6.6 that was purged with CO_2, which is the same electrolyte as was used for the photocathode. An anodic photocurrent was clearly observed, as in the cases of the aqueous solutions of Na_2SO_4 (pH 8) and $NaHCO_3$ (pH 8.3), that were both purged with Ar.[46] In addition, the evolution of O_2 under visible-light irradiation in a 50 mM aqueous solution of $NaHCO_3$ purged with CO_2 was confirmed by the analysis of the gas products at an applied potential of +0.2 V *vs.* Ag/AgCl, and its total faradaic efficiency was 93% after irradiating for 60 min (Fig. S9†).

Fig. 8 shows a schematic representation of the hybrid photoelectrochemical cell consisting of the **RuRe**/$CuGaO_2$ photocathode and the CoO_x/TaON photoanode in a *Z*-scheme configuration. Two chambers containing the electrolyte solution purged with CO_2 were separated by a Nafion membrane, and one photoelectrode was installed in each chamber. Visible light with λ_{ex} > 460 nm and λ_{ex} > 400 nm was used to irradiate the **RuRe**/$CuGaO_2$ photocathode and the CoO_x/TaON photoanode, respectively. It is worth nothing that the photoelectrochemical reaction was conducted under short-circuit conditions with the same electrolyte for both electrodes, *i.e.*, there was no external electrical or chemical bias between the electrodes. In addition, a higher intensity of irradiated light was utilized for the photocathode (4.5×10^{17} photon cm^{-2} s^{-1} in the wavelength range 460–600 nm) than that for the photoanode (4.1×10^{16} photon cm^{-2} s^{-1} in the wavelength range 400–600 nm) to achieve sufficient photoexcitation of the loaded **RuRe** on the photocathode.

Photoelectrolysis using the constructed photoelectrochemical cell was conducted with intermittent visible-

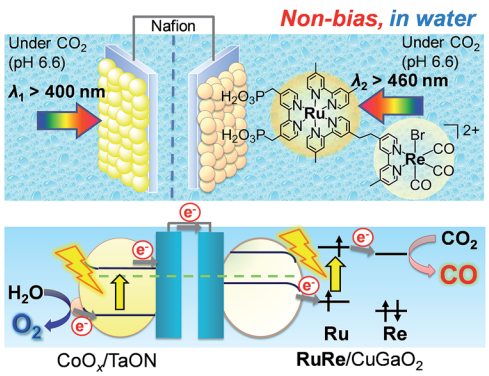

Fig. 8 Schematic image of the hybrid photoelectrochemical cell in a *Z*-scheme configuration.

light irradiation for a total of 2 h. Fig. 9 shows the time courses of the photocurrent and electrode potentials (a) and the chemical products (b). The generation of a photocurrent and a corresponding increase in the products were clearly observed under irradiation, and the working potential of the electrodes was confirmed to be around +0.15 V *vs.* Ag/AgCl, at which point both of the photoelectrodes could generate a photocurrent under irradiation *via* the respective half reactions. The products of the reduction (CO and H_2) and oxidation (O_2) were detected in the cathode and anode chambers, respectively (Fig. S10†). A total of 232 nmol of CO was produced, and the TON_{CO} reached 22 based on the amount of immobilized **RuRe** before the irradiation. The total faradaic efficiency of the cathodic reaction, including the evolution of H_2 (311 nmol), was 72%, whereas that of the anodic reaction was 70% (266 nmol O_2). Notably, an electron balance between the reduction products (CO and H_2) and the oxidation product (O_2) was almost acquired in this photoelectrochemical reaction, while in the case of the corresponding system using the NiO electrode instead of $CuGaO_2$, there were much less reduction products than the produced O_2.[32] The slight decrease in the half amount of electrons when the light was cut in Fig. 9(b) means that a reverse current flowed, which was possibly derived from the discharge of the electrical double layers of the electrodes. When only the cathode or the anode was irradiated, the photocurrent was relatively small in comparison to that when both of the electrodes were under irradiation (Fig. S11†), which suggests that photoexcitation of both of the electrodes is required for the subsequent progress of the photochemical reduction of CO_2 with water as the reductant. On the basis of these data, we conclude that this hybrid photoelectrochemical cell can drive both the reduction of CO_2 and the oxidation of water by the stepwise photoexcitation of **RuRe** and TaON, *i.e.*, *via Z*-scheme-type electron transfer, which gives CO and O_2 under visible-light irradiation. This is the first successful instance of the reduction of CO_2 in the absence of electrical or chemical bias using visible light and water alone by a hybrid photocatalytic system consisting of a molecular photocatalyst and a semiconductor photocatalyst. Further investigations for the improvement of the efficiency and durability of the photoelectrochemical cell are currently under way in our laboratory.

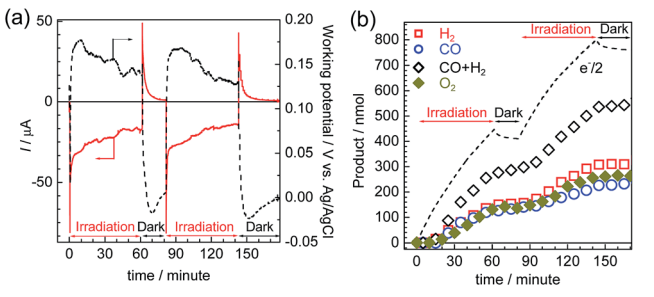

Fig. 9 Time courses of the photocurrent and working potential of the electrodes (a) and the chemical products (b) during the visible-light irradiation of the photoelectrochemical cell consisting of the RuRe/$CuGaO_2$ photocathode and the CoO_x/TaON photoanode under short-circuit conditions.

Experimental

Synthesis of $CuGaO_2$ particles

Particles of $CuGaO_2$ powder were prepared using a solid-state reaction method. The precursor materials, *i.e.*, Cu_2O (Kanto Chemicals, >92%) and Ga_2O_3 (Wako Chemicals, 99.99%), were mixed using an agate mortar. The molar ratio of the precursors was set at Cu : Ga = 1 : 1. The obtained mixture was calcined with a N_2 flow of 100 mL min^{-1} at 1373 K for 5 h to give a polycrystalline powder of $CuGaO_2$.

Fabrication of $CuGaO_2$ electrodes

Fluorine-doped tin oxide (FTO) glass (AGC Fabritech, 15 × 50 mm, 12 Ω sq^{-1}) was sonicated in acetone for 10 min and in methanol for 10 min before use. A suspension of 30 mg of $CuGaO_2$ powder in 300 μL of isopropanol was prepared with sonication for 10 min. Then, 100 μL of the suspension was dropped onto an exposed area of the FTO glass (*ca.* 5 cm^2) and dried in air at room temperature using a drop-casting method and Scotch mending tape as a masking material. The obtained sample was calcined at 773 K for 3 h with a N_2 flow of 100 mL min^{-1}. The electrode was cut in half before use. The amount of powder that was deposited was estimated to be approx. 5 mg for each electrode (*ca.* 2.5 cm^2).

Preparation of the hybrid photocathode by the adsorption of the metal complex on the $CuGaO_2$ electrode

RuRe and its model complexes (**Ru** and **Re**) (Chart 1) were synthesized in accordance with reported procedures.[43] A $CuGaO_2$ electrode was immersed in an acetonitrile solution containing the metal complex (4 mL, 5 μM) overnight. The electrode was washed with acetonitrile after the adsorption procedure. The amount of the metal complex that was adsorbed was estimated from the difference in the absorbance between the solutions at 461 nm before and after the hybridization procedures.

Preparation of the CoO_x/TaON photoanode

The CoO_x/TaON electrode was prepared in accordance with a reported procedure.[46] The outline of the procedure is as follows. TaON powder was prepared by heating Ta_2O_5 powder with an NH_3 flow (20 mL min^{-1}) at 1123 K for 15 h. CoO_x nanoparticles (5 wt% as the metal) were loaded onto the TaON particles *via* impregnation from an aqueous $Co(NO_3)_2$ solution, followed by heating at 673 K for 30 min in air. The as-prepared CoO_x-loaded TaON particles were deposited on a Ti substrate using electrophoretic deposition. The electrodes were treated with 50 μL of a solution of $TaCl_5$ in methanol (10 mM) and then dried in air at room temperature. After this process had been performed five times, the electrode was heated in an NH_3 flow (10 mL min^{-1}) at 723 K for 30 min. The details of the structural characterization of the electrode are shown in our previous paper.

Photoelectrochemical measurements and reduction of CO_2 using the RuRe/$CuGaO_2$ photocathode

A three-electrode setup with an HZ-7000 potentiostat (Hokuto Denko) was used throughout the photoelectrochemical measurements and half reactions. A 50 mM aqueous solution of $NaHCO_3$ saturated with CO_2 (pH 6.6) was used as an electrolyte. A Pt wire and Ag/AgCl in a saturated aqueous solution of KCl were employed as the counter and reference electrodes, respectively. The counter electrode was separated from the reaction solution using Vycor glass to avoid the influence of the oxidation reaction taking place on the counter electrode. The working electrode (*ca.* 2.5 cm^2) was irradiated using a 300 W Xe lamp (Asahi Spectra MAX-302) with an IR-blocking mirror module. A cutoff filter (HOYA Y48 for irradiation at $\lambda_{ex} > 460$ nm) or a band-pass filter (Asahi Spectra, for the IPCE measurements) was employed to control the irradiation wavelength. The potential against a reversible hydrogen electrode (RHE) (see Fig. 1) was calculated using the Nernst equation (eqn (1)):

$$E\ (\text{V } \textit{vs.}\ \text{RHE}) = E\ (\text{V } \textit{vs.}\ \text{Ag/AgCl}) + 0.199 + 0.059\ \text{pH}. \quad (1)$$

The dependence on the wavelength of the IPCE at a given wavelength was calculated using eqn (2):

$$\text{IPCE}\ (\%) = [(1240/\lambda_{ex})(I_{light} - I_{dark})/P_{light}] \times 100, \quad (2)$$

where λ_{ex} and P_{light} are the wavelength and power density of the incident light (nm and $\mu W\ cm^{-2}$), respectively, I_{light} is the current density under irradiation ($\mu A\ cm^{-2}$), and I_{dark} is the current density in the dark ($\mu A\ cm^{-2}$).

The photoelectrochemical reduction of CO_2 was conducted using a Pyrex cell sealed with an O-ring and a stirring tip. The total volume of the cell without the stirring tip and electrodes was *ca.* 130 mL, and 84 mL of the electrolyte solution was utilized; therefore, the estimated volume of the gas phase was *ca.* 46 mL. The reaction was conducted after purging the system with CO_2 for more than 40 min. A cutoff filter (HOYA Y48) was employed for irradiation at $\lambda_{ex} > 460$ nm. Product analyses of CO and H_2 in the gas phase and HCOOH in the liquid phase were performed using a gas chromatograph (Inficon MGC3000A) and a Capi-3300I capillary electrophoresis system (Otsuka Electronics), respectively. $^{13}CO_2$ (CIL, $^{13}C = 99\%$) and $NaH^{13}CO_3$ (Aldrich, $^{13}C = 99\%$) were utilized for the labeling experiments. Gas chromatography-mass spectrometry (GC-MS) analysis of the gas phase was conducted using a gas chromatograph equipped with a mass spectrometer (Shimadzu GCMS-QP2010 Ultra).

Photoelectrochemical reduction of CO_2 using the hybrid electrochemical cell in the *Z*-scheme configuration

The reaction was conducted using a Pyrex cell with two chambers (*ca.* 27 mL for each chamber) that were divided by a Nafion 117 membrane (Aldrich), and the photoelectrodes were installed into each chamber and the cell was sealed with an O-ring. Ag/AgCl in a saturated aqueous solution of KCl was employed as the reference electrode and was placed into the cathode chamber. A 14.5 mL portion of a 50 mM aqueous solution of $NaHCO_3$ was added as an electrolyte to each chamber, which was purged with CO_2. A three-electrode setup with an HZ-7000 potentiostat (Hokuto Denko) was used in non-resistance ammeter mode. The **RuRe**/$CuGaO_2$ photocathode (*ca.* 3.2 cm^2, **RuRe** 10.5 nmol) was irradiated at $\lambda_{ex} > 460$ nm using a 300 W Xe lamp (Eagle Engineering) with a cutoff filter (HOYA Y48) and a cold mirror (CM-1). The CoO_x/TaON photoanode (*ca.* 3.3 cm^2) was irradiated at $\lambda_{ex} > 400$ nm using a 300 W Xe lamp (Asahi Spectra MAX-302) with a cutoff filter (HOYA L42) and an IR-blocking mirror module. The analysis of gas products was performed using gas chromatography (Inficon MGC3000A).

Characterizations

UV-vis diffuse reflectance spectra were recorded using a V-565 spectrophotometer (JASCO) that was equipped with an integral sphere unit. X-ray diffraction (XRD) patterns were recorded using a MiniFlex600 X-ray diffractometer (Rigaku) that was equipped with monochromatic Cu Kα radiation and operated at 15 mA and 40 kV. The scanning electron microscopy (SEM) observations were conducted using an S-4700 microscope (Hitachi High-Tech). An ECSA-3400 X-ray photoelectron spectrometer (Shimadzu) was utilized for the X-ray photoelectron spectroscopy (XPS) measurements. The binding energies were corrected using the C 1s peak (284.6 eV) for each sample.

Conclusions

A novel hybrid photocathode consisting of a $CuGaO_2$ p-type semiconductor and a **RuRe** supramolecular complex has been developed for the photoelectrochemical reduction of CO_2 in aqueous solution. The **RuRe**/$CuGaO_2$ photocathode displayed photoelectrochemical activity for the conversion of CO_2 to CO in an aqueous electrolyte solution with an onset potential of +0.3 V *vs.* Ag/AgCl. A photoelectrochemical cell comprising the **RuRe**/$CuGaO_2$ photocathode and a CoO_x/TaON photoanode exhibited activity for the visible-light-driven reduction of CO_2 using water as a reductant to generate CO, H_2, and O_2 with no external bias.

Acknowledgements

This work was supported by JSPS KAKENHI Grant Number JP24107005 in Scientific Research on Innovative Areas "Artificial Photosynthesis (AnApple)", the Strategic International Collaborative Research Program (SICORP) from JST, and JST CREST Grant Number JPMJCR13L1 in "Molecular Technology". H. K. thanks JSPS KAKENHI Grant Number JP16K21031 for Young Scientists (B) and K. M. thanks JSPS KAKENHI Grant Number JP16H06441 in Scientific Research on Innovative Areas "Mixed Anion" for their financial support. We thank Prof. Kazunari Domen from the University of Tokyo for the SEM measurements.

Notes and references

1 A. J. Morris, G. J. Meyer and E. Fujita, *Acc. Chem. Res.*, 2009, **42**, 1983–1994.
2 G. Sahara and O. Ishitani, *Inorg. Chem.*, 2015, **54**, 5096–5104.
3 Y. Yamazaki, H. Takeda and O. Ishitani, *J. Photochem. Photobiol., C*, 2015, **25**, 106–137.
4 A. Nakada, K. Koike, T. Nakashima, T. Morimoto and O. Ishitani, *Inorg. Chem.*, 2015, **54**, 1800–1807.
5 A. Nakada, K. Koike, K. Maeda and O. Ishitani, *Green Chem.*, 2016, **18**, 139–143.
6 B. Gholamkhass, H. Mametsuka, K. Koike, T. Tanabe, M. Furue and O. Ishitani, *Inorg. Chem.*, 2005, **44**, 2326–2336.
7 S. Sato, K. Koike, H. Inoue and O. Ishitani, *Photochem. Photobiol. Sci.*, 2007, **6**, 454–461.
8 K. Koike, S. Naito, S. Sato, Y. Tamaki and O. Ishitani, *J. Photochem. Photobiol., A*, 2009, **207**, 109–114.
9 Y. Tamaki, T. Morimoto, K. Koike and O. Ishitani, *Proc. Natl. Acad. Sci. U. S. A.*, 2012, **109**, 15673–15678.
10 Y. Tamaki, K. Watanabe, K. Koike, H. Inoue, T. Morimoto and O. Ishitani, *Faraday Discuss.*, 2012, **155**, 115–127.
11 Y. Tamaki, K. Koike, T. Morimoto and O. Ishitani, *J. Catal.*, 2013, **304**, 22–28.
12 Y. Tamaki, K. Koike, T. Morimoto, Y. Yamazaki and O. Ishitani, *Inorg. Chem.*, 2013, **52**, 11902–11909.
13 E. Kato, H. Takeda, K. Koike, K. Ohkubo and O. Ishitani, *Chem. Sci.*, 2015, **6**, 3003–3012.
14 Y. Tamaki, K. Koike and O. Ishitani, *Chem. Sci.*, 2015, **6**, 7213–7221.
15 T. Arai, S. Sato, K. Uemura, T. Morikawa, T. Kajino and T. Motohiro, *Chem. Commun.*, 2010, **46**, 6944.
16 S. Sato, T. Arai, T. Morikawa, K. Uemura, T. M. Suzuki, H. Tanaka and T. Kajino, *J. Am. Chem. Soc.*, 2011, **133**, 15240–15243.
17 T. Arai, S. Tajima, S. Sato, K. Uemura, T. Morikawa and T. Kajino, *Chem. Commun.*, 2011, **47**, 12664–12666.
18 T. Arai, S. Sato, T. Kajino and T. Morikawa, *Energy Environ. Sci.*, 2013, **6**, 1274–1282.
19 K. Maeda, K. Sekizawa and O. Ishitani, *Chem. Commun.*, 2013, **49**, 10127–10129.
20 K. Maeda, R. Kuriki, M. Zhang, X. Wang and O. Ishitani, *J. Mater. Chem. A*, 2014, **2**, 15146–15151.
21 T. Arai, S. Sato and T. Morikawa, *Energy Environ. Sci.*, 2015, **8**, 1998–2002.
22 R. Kuriki, K. Sekizawa, O. Ishitani and K. Maeda, *Angew. Chem., Int. Ed.*, 2015, **54**, 2406–2409.
23 K. Maeda, R. Kuriki and O. Ishitani, *Chem. Lett.*, 2016, **45**, 182–184.
24 R. Kuriki, O. Ishitani and K. Maeda, *ACS Appl. Mater. Interfaces*, 2016, **8**, 6011–6018.
25 K. Sekizawa, K. Maeda, K. Domen, K. Koike and O. Ishitani, *J. Am. Chem. Soc.*, 2013, **135**, 4596–4599.
26 F. Yoshitomi, K. Sekizawa, K. Maeda and O. Ishitani, *ACS Appl. Mater. Interfaces*, 2015, **7**, 13092–13097.
27 A. Nakada, T. Nakashima, K. Sekizawa, K. Maeda and O. Ishitani, *Chem. Sci.*, 2016, **7**, 4364–4371.
28 R. Kuriki, H. Matsunaga, T. Nakashima, K. Wada, A. Yamakata, O. Ishitani and K. Maeda, *J. Am. Chem. Soc.*, 2016, **138**, 5159–5170.
29 K. Muraoka, H. Kumagai, M. Eguchi, O. Ishitani and K. Maeda, *Chem. Commun.*, 2016, **52**, 7886–7889.
30 K. Wada, M. Eguchi, O. Ishitani and K. Maeda, *ChemSusChem*, 2017, **10**, 287–295.
31 G. Sahara, R. Abe, M. Higashi, T. Morikawa, K. Maeda, Y. Ueda and O. Ishitani, *Chem. Commun.*, 2015, **51**, 10722–10725.
32 G. Sahara, H. Kumagai, K. Maeda, N. Kaeffer, V. Artero, M. Higashi, R. Abe and O. Ishitani, *J. Am. Chem. Soc.*, 2016, **138**, 14152–14158.
33 J. He, H. Lindström, A. Hagfeldt and S.-E. Lindquist, *J. Phys. Chem. B*, 1999, **103**, 8940–8943.
34 N. Kaeffer, J. Massin, C. Lebrun, O. Renault, M. Chavarot-Kerlidou and V. Artero, *J. Am. Chem. Soc.*, 2016, **138**, 12308–12311.
35 S. Nandy, A. Banerjee, E. Fortunato and R. Martins, *Rev. Adv. Sci. Eng.*, 2013, **2**, 273–304.
36 H. Kawazoe, M. Yasukawa, H. Hyodo, M. Kurita, H. Yanagi and H. Hosono, *Nature*, 1997, **389**, 939–942.
37 H. Yanagi, H. Kawazoe, A. Kudo, M. Yasukawa and H. Hosono, *J. Electroceram.*, 2000, **4**, 407–414.
38 K. Ueda, T. Hase, H. Yanagi, H. Kawazoe, H. Hosono, H. Ohta, M. Orita and M. Hirano, *J. Appl. Phys.*, 2001, **89**, 1790–1793.
39 A. Renaud, B. Chavillon, L. Le Pleux, Y. Pellegrin, E. Blart, M. Boujtita, T. Pauporté, L. Cario, S. Jobic and F. Odobel, *J. Mater. Chem.*, 2012, **22**, 14353–14356.
40 M. Yu, G. Natu, Z. Ji and Y. Wu, *J. Phys. Chem. Lett.*, 2012, **3**, 1074–1078.
41 J. W. Lekse, M. K. Underwood, J. P. Lewis and C. Matranga, *J. Phys. Chem. C*, 2012, **116**, 1865–1872.
42 M. Lee, D. Kim, Y. T. Yoon and Y. Il Kim, *Bull. Korean Chem. Soc.*, 2014, **35**, 3261–3266.
43 Y. Ueda, H. Takeda, T. Yui, K. Koike, Y. Goto, S. Inagaki and O. Ishitani, *ChemSusChem*, 2015, **8**, 439–442.
44 The value of $E^{*\mathrm{red}}_{1/2}$ of **RuRe** was calculated using the reported values of $E^{\mathrm{red}}_{1/2}$ and E_{00} from ref. 31 and was converted to potential *vs.* Ag/AgCl.
45 Y. Kuramochi and O. Ishitani, *Inorg. Chem.*, 2016, **55**, 5702–5709.
46 M. Higashi, K. Domen and R. Abe, *J. Am. Chem. Soc.*, 2012, **134**, 6968–6971.